CHIRALITY 12:191–198 (2000)

Vibrational Circular Dichroism of Tetraphenylporphyrin in Peptide Complexes? A Computational Study

PETR BOUŘ,[1,2]* KAMIL ZÁRUBA,[1] MARIE URBANOVÁ,[3] VLADIMÍR SETNIČKA,[1] PAVEL MATĚJKA,[1] ZDENĚK FIEDLER,[2] VLADIMÍR KRÁL,[1] AND KAREL VOLKA[1]

[1]*Department of Analytical Chemistry, Institute of Chemical Technology, Prague, Czech Republic*
[2]*Institute of Organic Chemistry and Biochemistry, Academy of Sciences of the Czech Republic, Prague, Czech Republic*
[3]*Department of Physics and Measurement, Institute of Chemical Technology, Prague, Czech Republic*

ABSTRACT The Raman and absorption spectra of tetraphenylporphyrin (TPP) were calculated and compared to experiment. The computation was based on the harmonic molecular force field and electric tensors obtained ab initio at the BPW91/6-31G* level. Good agreement was found between experimental and calculated frequencies and intensities. In order to estimate whether induced optical activity in chiral complexes interferes with the signal of peptide vibrations, the vibrational circular dichroism (VCD) spectra of TPP were simulated. The magnetic field perturbation theory (MFP) and the gauge-invariant atomic orbitals (GIAO) were used for the simulation. Such spectra were compared to theoretical VCD intensities of a model tripeptide as well to experimental spectra of a complex of the peptide and tetrakis(*p*-sulfonatophenyl)porphyrin (TSPP). No significant contribution to VCD signal from the TPP residue was found in experimental spectra. Thus, possible peptide conformational changes occurring during the complexation can be monitored directly in the amide I frequency region. *Chirality 12:191–198, 2000.*

KEY WORDS: Raman; infrared; vibrational circular dichroism; ab initio; chiral complexes

Porphyrin derivatives have been widely used in spectroscopy because of their low cost and interesting chemical and light-scattering properties.[1,2] Understanding their behavior is important both for industrial applications and in vitro studies of the living matter.[3,4] Recently, advances in computational chemistry enabled direct ab initio modeling of molecules of similar size. This is important for the interpretation of the vibrational optical activity, which is based primarily on quantum-chemical modeling.[5] Many spectroscopic properties can be derived from the symmetry rules for the D_{2h} symmetry of the porphyrin skeleton, which often adopts even higher D_{4h} symmetry in metal complexes. Perturbations of this symmetry by interaction with a chiral environment may lead to optical activity. For example, magnetic circular dichroism arises when the molecule is placed into a magnetic field.[6] In this study, symmetry perturbation for tetraphenylporphyrin (TPP, see Fig. 1) caused by a chiral ligand is considered.

We conducted several spectroscopic studies of peptide complexes with various TPP derivatives.[7,8] Recently, we also adopted the vibrational circular dichroism (VCD) technique. Other experiments confirmed that the porphyrin residue may intercalate into DNA molecules. Such phenomena can also be studied by VCD spectroscopy.[9] Thus, we find it important to investigate porphyrin vibrational properties in detail. Although the TPP moiety is not optically active, induced chirality in the complexes with chiral compounds can interfere with the signal. In this study we simulated the magnitude and frequency range of possible VCD signals of the TPP chromophore. Conformational dependence of vibrational spectra was compared for absorption, Raman, and VCD intensities.

Tetraphenylporphyrin derivatives can be easily prepared and their vibrational properties have been widely explored in spectroscopic studies.[10] For example, resonance and nonresonance Raman spectroscopic studies are very sensitive to minor changes in molecular structure.[11,12] However a complete vibrational analysis for such systems is hindered by their relatively large size. Simplified models using empirical potentials are regularly adopted.[13] A detailed normal mode analysis was done for the porphyrin residue.[14] Thus, we consider a priori assignment of the vibrational modes in the tetraphenylporphyrin molecule as the next logical step in these studies.

Contract grant sponsors: the Grant Agency of the Czech Republic; the Ministry of Education of the Czech Republic; Contract grant numbers: 203/97/P002; VS97135.
*Correspondence to: Dr. Petr Bouř, Institute of Organic Chemistry and Biochemistry, Academy of Sciences of the Czech Republic, Flemingovo nam 2, 16610, Praha 6, Czech Republic. E-mail: bour@uochb.cas.cz
Received for publication 16 September 1999; Accepted 30 November 1999

TABLE 1. List of the TPP conformers

Name	Energy [kcal/mol]	Symmetry	ϕ_1[a]	ϕ_2[a]	ϕ_3[a]	ϕ_4[a]	Population[b] [%]
tlrrl	1.4	C_{2h}	−67	67	67	−67	12.5
trrll	1.2	C_{2h}	70	70	−70	−70	12.5
trlrr	0.3	C_1	68	−65	68	70	25 + 25*
trrrr	0.6	D_2	70	70	70	70	6.25 + 6.25*
trlrl	0	C_{2v}	65	−65	65	−65	12.5
tpp[c]	1.3	D_{2h}	90.0	90.0	90.0	90.0	—

*Denotes the enantiomer.
[a]Angles between the phenyl and porphyrin planes (small deviations from planarity in both chromophores was neglected), see Figure 1.
[b]Statistical populations without Boltzmann weighting.
[c]Transition structure, with four imaginary frequencies in the range of i25–i29 cm^{-1}.

COMPUTATIONS

Program Gaussian[15] was used for all ab initio computations. Molecular geometries were obtained by the energy minimization at the BPW91/6-31G* level (comprising the Becke and Perdew-Wang density functionals[16,17]) with the default parameters of Gaussian. The absorption and VCD spectra were calculated at the same level of approximation, the latter using the gauge-invariant atomic orbital (GIAO) and the magnetic field perturbation theory (MFP).[18,19] Raman spectra were obtained via a Cartesian transfer[20] of the polarizability derivatives calculated at the HF/6-31G* level to the optimized geometries. A similar procedure was adopted for smaller fragments, as specified below.

EXPERIMENTAL

The absorption IR spectrum of TPP was measured with a Nicolet FTIR spectrometer in a KBr pellet using a resolution of 2 cm^{-1}. Back-scattered Raman spectrum was obtained with a polycrystalline sample using a laser excitation wavelength of 1064 nm (Bruker Equinox 55/S spectrometer, 256 scans, resolution of 2 cm^{-1}). VCD and absorption spectra of the sodium salt of tetrakis(*p*-sulfonatophenyl)-porphyrin (TSPP) and peptide (L-Lys-Ala-Ala-$OCH_3 \cdot (HBr)_2$, LAA) complexes were recorded using a Bruker IFS 66/S spectrometer equipped with the VCD/IRRAS PMA 37 module, using a resolution of 8 cm^{-1}. Peptide concentration in D_2O was kept constant (13.5 mM), optical path length was 25 μm.

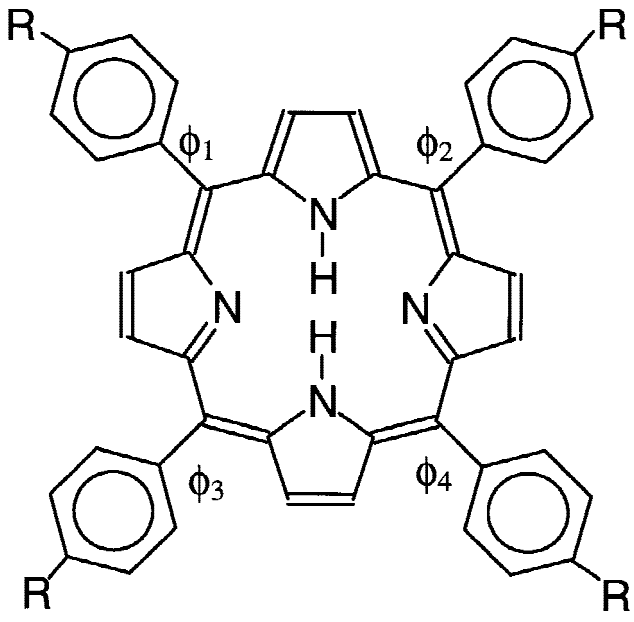

Fig. 1. Tetraphenylporphyrin (TPP, R=H) or tetrakis(*p*-sulfonatophenyl)porphyrin (TSPP, R=SO_3H) with the four bonds exhibiting restricted rotation.

RESULTS AND DISCUSSION

Geometry of TPP

In the spatially most convenient D_{2h} conformation, the phenyl groups are perpendicular to the porphyrin plane. However, a less symmetric arrangement was observed in X-ray experiments both for the tetragonal[21] and triclinic[22] forms of TPP. Although this can be conventionally attributed to the stabilizing effect of a partial π-electron conjugation, a low-level HF/4-31G test computation did not provide other than the perpendicular (D_{2h}) conformer. On the other hand, the more advanced BPW91/6-31G* energy minimization leads to the multiple equilibrium geometries summarized in Table 1, but not to the fully symmetric D_{2h} structure. This different behavior of the two ab initio models may be partially attributed to the influence of the electron correlation for porphyrin properties, as pointed out previously.[23] Note that the correlation is partially included in the BPW91 functional. The trlrl and tlrrl forms (see Table 1) correspond to TPP conformations found in tetragonal and triclinic crystals, respectively.

Since the calculated relative conformer energies are small, independent rotation of the phyenyl group within the range of 90 ± 25° can be expected for a free TPP molecule in a solvent. Conformational ratios obtained with this assumption are given in the last column of Table 1. Quite a low rotational barrier corresponding to the transition structure (tpp) was found at the BPW91/6-31G* level with "imaginary" saddle-point frequencies smaller than 30 cm^{-1}. Because of this virtually free motion of the phenyl groups, the two optically active forms (trrrr, trlrr) can be stabilized in complexes with chiral ligands with a low energy cost. However, as shown below, its VCD signal was not found in our spectra because of its low magnitude.

For the triclinic crystalline form of TPP a significant non-

TABLE 2. CPU computer times for force field computation, in hours

Conformer	Symmetry	BPW91/6-31G*[a]	HF/6-31G*[a]
tlrrl	C_{2h}	36	80
trrll	C_{2h}	34	71
trlrr	C_1	121	
trrrr	D_2	39	83
trlrl	C_{2v}	39	79
tpp[c]	D_{2h}	30	65

[a]With default parameters of Gaussian 98, HF calculation includes an additional analytical estimation of polarizability derivatives.
Times for the HP 9000/800 V-server, 240 MHz 8200 CPUs, 4-processor parallel run.

planarity of the porphyrin part was observed.[22] Pyrroles that do not carry hydrogens are almost coplanar, while the other pair is inclined by about 6°. The deviation was reproduced by the computation also for the tlrrl conformer, which suggests that the molecule is relatively weakly bound in the crystal, where the phenyl groups prevent stacking and further interaction of the porphyrin system. The observed nonplanarity is slightly greater than predicted for the molecule in vacuo; for example, the two center hydrogen atoms are by about 0.13 Å above and under the porphyrin plane for tlrrl, while a deviation of 0.16 Å was found by the X-ray method.

The computational times as given in Table 2 may be interesting from the practical point of view. Clearly, implementation of the symmetry reduces computational time approximately by two-thirds for all conformers, if compared to the "nonsymmetric" trlrr structure. Rather surprisingly, the trivial HF-SCF method scales very inefficiently in Gaussian 98 when compared to the more advanced DFT, perhaps because of the additional estimation of the polarizability derivatives.[15] These could not be obtained for the **trlrr** conformer because of excessive demands on the computer time and disk space.

Normal Mode Assignment for TPP

The assignment is based on the comparison of calculated and experimental absorption and Raman spectra of TPP. The spectra are plotted in Figure 2 for the trrrr conformer. The simulated Raman spectra were multiplied by an empirical factor of $\omega^{-3/5}$ in order to better match the experimental intensity profile. Because of the large number of normal modes (3N – 6 = 228), vibrational assignment was based on comparison of simulated and experimental spectral peaks, rather than on individual modes. Description of the normal modes based on their dynamic visualization is given in Table 3. Detailed computer output is available upon request.

The high-energetic N–H and C–H vibrations were calculated with higher frequencies than found by experiment, in accord with a previous experience for such ab initio modeling.[24,25] The systematic error of about 3% can be partially attributed to anharmonic interactions[26] and the influence of the solvent.[24] Relative band intensities are sufficiently reproduced by the simulation both for the absorption and Raman spectra, as can be compared in Figure 2.

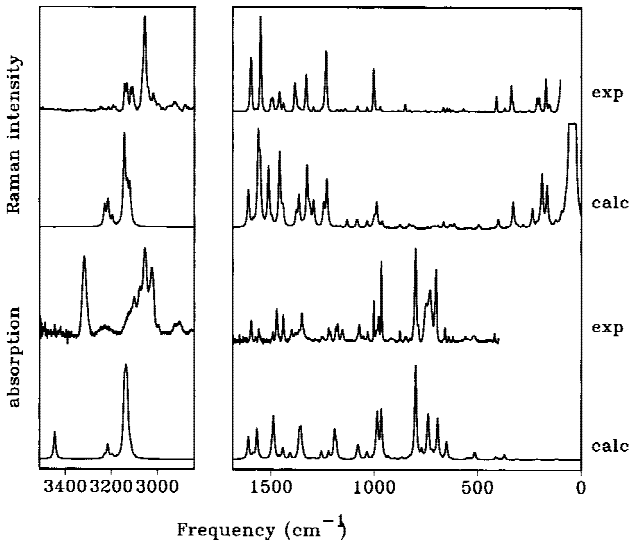

Fig. 2. Raman (top) and absorption (b0ttom) experimental and calculated spectra of TPP. Calculated Raman intensities in the mid ir region were multiplied by an empirical factor of $\omega^{-1.5}$, where ω is the transitional frequency.

In the mid- and low-frequency region, both the relative and absolute frequency errors diminish and quite realistic overall intensity patterns are obtained with the calculation. Most of the modes can be localized at the phenyl or porphyrin chromophores, as can be verified by the dynamic displacement visualization. Thus, a rather limited mechanical coupling is mediated by the single covalent bonds between these two chromophores.

Figure 3 shows the simulated conformational dependence of absorption and Raman spectra for the four symmetric conformers of TPP (tlrrl, trrll, trrrr, and trlrl). Raman spectra of the trlrr conformer could not be obtained with available computers. Interestingly, while absorption intensities significantly differ only in a limited frequency region and relative intensity changes are typically less than 10%, variations of the Raman intensities are often bigger than 50% and occur throughout the entire spectral region. This is in accord with the common knowledge that Raman spectra are more sensitive to conformational changes because of the local symmetry rules.[27] Observed frequencies and assignments are in agreement with the previous assignment based on resonance Raman spectra of TPP derivatives.[28] As indicated by the experiments, the porphyrin and TPP spectral patterns are relatively stable and can be found in the derived compounds. The stability reflects the compactness and mutual mechanical isolation of the phenyl and porphyrin π-electron systems in the molecule.

As indicated in the Introduction, induced optical activity of the TPP residue can be expected in complexes with chiral ligands. In this study we have restricted ourselves only to the chirality mediated by conformational changes, since its contribution is presumably the largest. The simulated VCD spectra for the two optically active forms (trrrr and trlrr) are plotted in Figure 4. Apparently, the spectrum of trrrr is approximately that of trlrr multiplied by a factor of two. This reflects the local nature of VCD, stemming

TABLE 3. Assignment of TPP spectral bands

Mode	ω_{sim}	ω_{IR}	ω_{Ram}	
1–2	3447	3323	3323	N–H stretch
3–10	3230	3099	3144	C–H stretch, in porphyrin
	3215	3079	3133	
	3197	3060	3117, 3109	
11–30	3145	3054	3055	C–H stretch, in phenyls
	3138	3010		
	3132		3041	
	3122		3018	
31–38	1610	1598	1597	C=C stretch, phe
	1587	1574	1574	
39–45	1569	1559		C=C stretch, por
	1554		1551	
	1513	1506	1502	
46–49	1497		1493	CH bend, phe
50–53	1489	1474		C=C stretch, in por
	1459	1458	1460	
54–57	1445	1443	1440	CH bend, phe
58–60	1408	1401	1410	CH bend, por
	1378		1385	
	1366		1376	
61–63	1363	1364		C–N stretch
	1355	1351		
64–67	1345	1342		CH bend, phe
68–76	1326		1329	CH bend
	1315		1318	
	1294		1295	
	1291	1288		
	1256	1250	1256	
77	1246	1250	1250	CH bend, C–N stretch
78–79	1230		1233	C–C stretch, por
80–82	1193	1187		CH bend, por
83	1190			NH bend
84–91	1184	1178	1180	CH bend, phe
	1164		1162	
92	1133		1141	NH bend
93–104	1082		1081	CH bend, complex
	1079	1073		
	1035	1033	1035	
105	1007			breathing, por
106–116	1000		1004	deformation of por skel.,
	989		1004	also pyrrole breathing
	985	980		
	966	966		
	963		971	
117–128	932		943	CH out of plane, phe
	901		913	
129–130	882			CH out of plane, por
131	876		884	breathing, por
132–134	867	877	872	CH out of plane, por
135–136	865–856			phenyl deaf
137–140	833–832		851	CH out of plane, phe
141–144	812		829	CH out of plane, phe
145	800			CH out of plane, por
149–157	744		752	out of plane deformation
	720	722	725	of por
158–161	693	701		oop def., phe
162	679			NH oop bend, out of phase
163	666		666	oop def., por
164	662			in plane def., por
165	660			oop def., por
166–167	652	660		ip def., por
168	634		649	oop def., por
169	631	636	636	ip def., por
170–182	615		621	oop def., por
	555		567	
	550	559		
	538	546		
	534		540	
	512	520		
	495		492	
183–185	436–412			ip def., por
186–189	402–400			oop def., phe
190	388			ip def., por
191	372			oop def., por
192–193	355		368	ip def., por
194–198	329		338	oop def., por
	308		330	
	279		295	
200–207	235		213	phenyl wagging
	215		203	
208	189		171	skeletal breathing
209	175			def. skel.
210–217	165		154	skel. def., por
218–228	52–9			phenyl wagging and rotation, molecular def.

ω_{sim}, simulated maxima of spectral signals; based on the trrrr calculation, see Fig. 2; oop, out-of-plane; ip, in-plane vibration.

primarily from the interaction of the phenyl and porphyrin chromophores. In the trlrr conformer two phenyl groups are twisted by angles of opposite signs and their contributions to the VCD spectrum mutually cancel. Relatively small intensity of VCD has important implications for further modeling. Since the VCD signal primarily rises from the local chirality in the vicinity of the rotating bonds, similar properties can be extended for other TPP derivatives. Generally, the low intensity can be considered both as an obstacle (when TPP is functioning as a chiral probe) as well as an advantage (when the interferene of the VCD signal from TPP is not desired).

TSPP Derivative

The tetrakis(*p*-sulfonatophenyl)porphyrin · Na_4 (TSPP · Na_4) molecule is widely used for complexation studies with biomolecules.[29] It is soluble in water due to the presence of

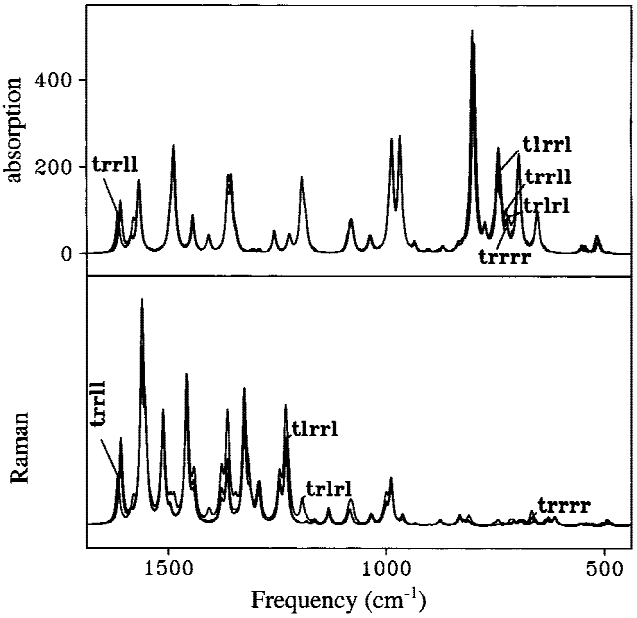

Fig. 3. Simulated conformational dependence of Raman and absorption spectra for four conformers of TPP, see Table 1.

the polar sulfo groups. Since it contains the TPP residue, the expected optical activity of its conformer can be estimated on the basis of the simulations for the TPP molecule. The sulfo- groups are both mutually isolated and oriented symmetrically, so that no chiral coupling between them can be expected.[27,30] Given the local C_3 symmetry of the SO_3^- groups and the semi-free rotating S–C bond, its local chirality is supposedly small.

In order to test whether the results obtained for TPP are also applicable for the sulfonated derivative, we calculated absorption spectra of the TSPP compound in the D_{2h} conformation. Theoretical studies of other conformations were not computationally feasible. In Figure 5, the absorption spectrum of TSPP obtained is compared to TPP (the tpp conformer) and experimental spectrum of TSPP. The spectra in the figure are plotted in the same scale. Apparently, the simulated signal of the modes that can be assigned to the TPP residue is very similar both in TPP and TSPP molecules. This was confirmed by the dynamic displacement of normal modes in both molecules. Thus, presumably the SO_3^- residues do not interact with the TPP core and hence do not significantly influence its optical activity. Unfortunately, agreement with experimental spectra of TSPP is very poor. This is caused by the difficulties associated with ab initio modeling of the force field of the sulfo group as well as a partial dissociation and possible stacking of the TSPP residues.[28] Also, computed second derivatives are heavily dependent on the basis set and approximation used, as indicated by the trial computations summarized in Table 4. For example, the frequencies for $CH_3SO_3^-$ obtained with the HF model are greater by about 140 cm^{-1} than those computed by DFT. This indicates that the current approximation is not adequate for precise modeling of the SO_3 vibrational modes. Moreover, the charged sulfo group interacts strongly with the solvent and baseline could not be fully subtracted for concentrated solutions used in the VCD measurement. Nevertheless, it may be concluded that normal modes located on the sulfo groups do not significantly mix with those of the TPP residue and thus have a minor influence on its VCD signal.

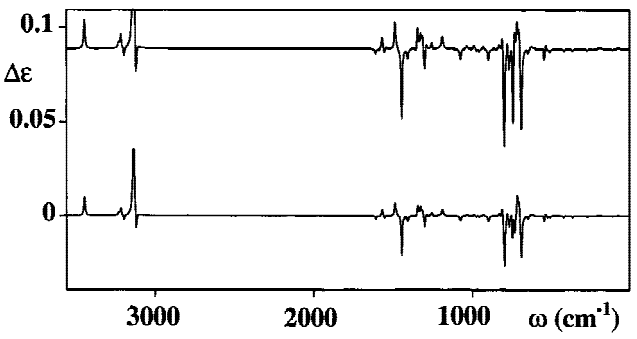

Fig. 4. Simulated VCD spectra of the two optically active conformers of TPP, trrrr (top) and trlrr (bottom).

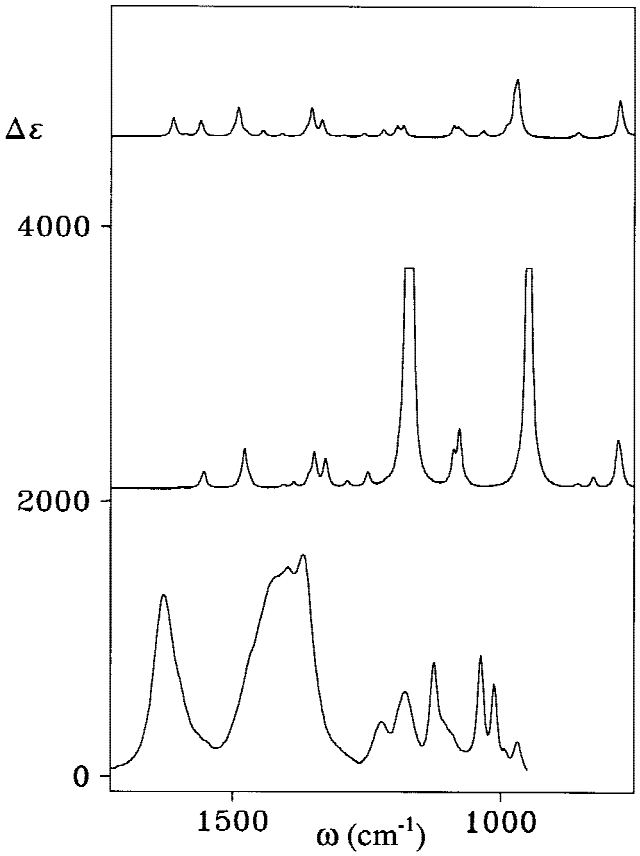

Fig. 5. Simulated absorption spectra of TPP (top), TSPP (middle) and experimental spectrum of TSPP (bottom).

Peptide-TSPP Complexes

Experimental absorption and VCD spectra of the complex of LAA and TSPP · Na_4 are plotted in Figure 6. The

TABLE 4. Dependence of calculated S=O stretching frequencies on the approximation used

System/approximation	ω (cm^{-1}) In phase	Out of phase
TSPP/BPW91-631G*	947	1,175
$CH_3SO_3^-$/HF-631G**	1,126	1,348
$CH_3SO_3^-$/BPW91-631G**	962	1,185
$CH_3SO_3^-$/B3LYP-631G**	1,001	1,224
CH_3SO_3H/B3LYP-631G**	1,121	1,350
$CH_3SO_3^-$/B3LYP-631G	768	885

absorption signal is clearly obscured by the absorption of TSPP, interferring with the amide I vibrations of the peptide.[31] The experimental changes in the intensity and shape of VCD spectra are about 10 times bigger than possible activity of the TPP residue (c.f. Fig. 4). Note also that the VCD intensity in Figure 4 is simulated for pure conformers, a situation that will not occur in real samples. Additionally, the presence of the isodichroic point at the experimental spectra at 1,633 cm^{-1} supports the idea that the changes can be attributed solely to the peptide molecule without interference from TSPP.

To test the reliability of the simulations, VCD spectra of LAA were simulated with the L-CH_3-(NHCO-C(CH_3)H-)$_2$-NHCO-CH_3 model tripeptide (AAA) at the same level of approximation (BPW91/6-31G*/MFP/GIAO) as for TPP. Additionally, the torsion angles were restricted in order to mimic the α-helical (ϕ = −57°, ψ = −47°), 3_{10}-helical (ϕ = −60°, ψ = −30°), random (polyproline II) (ϕ = −78°, ψ = 149°) and β-sheet (ϕ = −128°, ψ = 124°) conformations. VCD and absorption spectra for these systems were simulated (Fig. 7). Calculated amide I vibrations are shifted by about 100 cm^{-1} to higher frequencies, with respect to experimental values. Such errors in frequencies, however, do not significantly affect the shapes of the VCD patterns.[24–26,32] We can observe that the magnitude of intensity changes for different conformations is similar to the changes in observed spectra (c.f. Fig. 6). Moreover, comparison between the simulated and experimental spectra suggest that conformational transition of the peptide main chain may occur during complex formation. The negative VCD signal at higher frequencies may correspond to a presence of 3_{10}-helix in the free tripeptide. Note, that the peptide is not long enough for a proper α-helical conformation requiring the 1–4 amide-amide hydrogen binding. After the addition of TSPP, the negative VCD intensity shifts to lower frequencies and diminishes, which could signal a more extended form of the peptide chain close to the β-sheet structure. Presumably, the two $-NH_3^+$ groups in LAA bind to two sulfo- groups of TSPP, which destabilizes the compact "helical" form of the free tripeptide. The negative charges of the two free remaining sulfo- groups also repel the terminal $-COO^-$ residue of LAA. All the groups should be fully dissociated. Detailed analysis and further peptide complexes with TPP derivatives will be published separately.

With respect to the main topic of this study, it is interesting to compare the origin of the optical activity in peptides and the TPP residue. In the first case, the region of amide I is dominated by the dipolar interaction of the C=O groups, mechanically coupled trough the peptide main chain.[31] On the contrary, vibrations isolated on the phenyl group cannot be mutually mechanically coupled over the long distance in TPP and their VCD signal is small (e.g., modes 31–49). Relatively larger signal in the TPP residue is raised by the coupling of the C–C stretching vibration involving the $-CH_2-$ bridge in the porphyrin part (modes 50–57), since it is coupled with the C–C–C bending with the rotating single bonds.

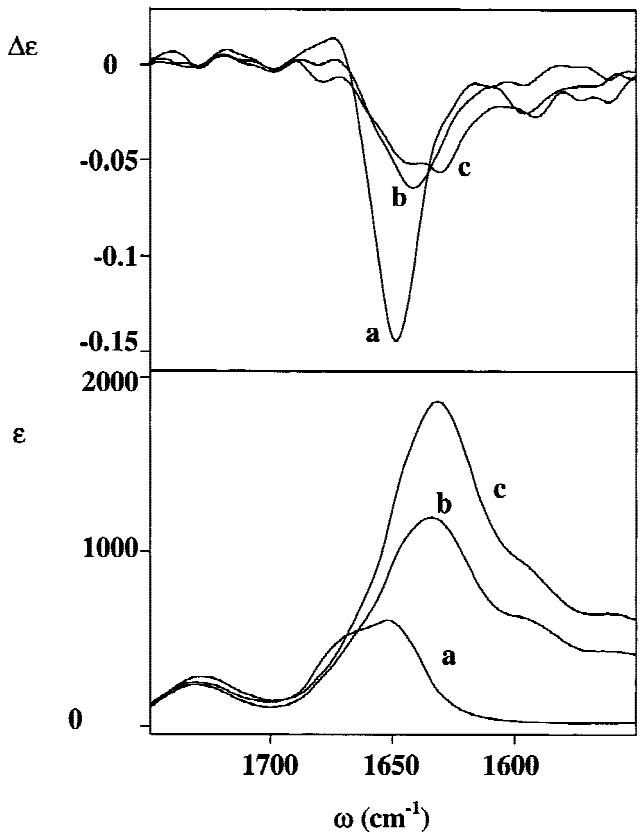

Fig. 6. Experimental spectra of the peptide-TSPP complexes for three molar ratios (TSPP/LAA): $\nu = 0$ (a), $\nu = 0.6$ (b) and $\nu = 0.9$ (c). Top – VCD, bottom – absorption. Concentration of LAA was kept constant during the measurement (13.5 mM, in D_2O).

CONCLUSION

Good agreement between simulated and experimental absorption and Raman spectra of TPP was found. Raman spectra were found to be more sensitive to molecular conformational changes than the absorption. The calculations predict almost free rotation of the phenyl groups in the TPP molecule for torsion angles in the range of 90 ± 25°. Simulated VCD spectra suggest that experimental intensities of the peptide–TPPS complexes do not contain a detectable contribution from the TPSS molecule. Thus, observed changes could be interpreted as conformational changes of the peptide component. It may be expected that

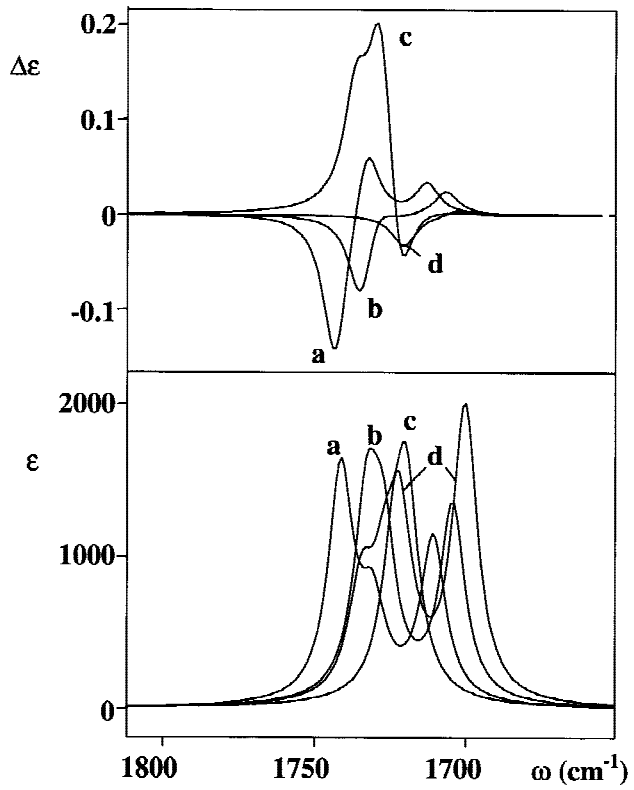

Fig. 7. Simulated VCD (top) and absorption (bottom) spectra of AAA in α-helical (a), 3_{10}-helical (b), random (c) and β-sheet (d) conformations. Simulations are based on a BPW91/6-31G** computations, for N-deuterated peptide.

the TPP moiety can be used as a chiral probe in the mid- and lower-frequency range in VCD experiment and, preferably, in Raman optical activity studies of the porphyrin–biomolecular complexes.

ACKNOWLEDGMENT

Computations were performed at the Supercomputer Center in Prague and at computer facilities of the University of Illinois at Chicago.

LITERATURE CITED

1. Smith KM. Porphyrins and metalloporphyrins. New York: Elsevier; 1975.
2. Doplin D. The prophyrins III, II. London: Academic Press; 1987.
3. Okamura MY, Feher G. Photosynthesis: energy conversion by plants and bacteria. New York: Academic Press; 1982.
4. Akins DL, Özçelik S, Zhu H, Guo C. Fluorescence decay kinetics and structure of aggregated tetrakis(*p*-sulfonatophenyl)porphyrin. J Phys Chem 1996;100:14390–14396.
5. Hester RE, Clark JH. Advances in spectroscopy, part B, vol 21. Chichester: John Wiley & Sons; 1993.
6. Pawlikowski M, Pilch M, Mortensen OS. Vibronic theory of magnetic vibrational circular dichroism in systems with fourfold symmetry: theoretical analysis for copper tetraphenylporphyrin. J Chem Phys 1992; 96:4982–4990.
7. Pančoška P, Urbanová M, Karvatovsky BN, Paschenko VZ, Vacek K. Fluorescence properties o tetraphenylporphyrin-polypeptide complexes as a model of photosynthetic systems. Chem Phys Lett 1987; 139:49–54.
8. Pančoška P, Urbanová M, Bednárová L, Vacek K, Vasilev S, Paschenko VZ, Maloň P, Král V. Model of porphyrin-protein complexes: tetraphenylporphyrine complexes with polycationic sequential polypeptides. Absorption, circular dichroism and fluorescence properties. Chem Phys 1990;147:401–413.
9. Maharaj V, Rauk A, van de Sande JH, Wieser H. Infrared absorption and vibrational circular dichroism spectra of selected deoxyoctanucleotides complexed with daunorubicin. J Mol Struct 1997;408–409: 315–318.
10. Akins DL, Guo C, Zhu H. Near-infrared-excited FT-Raman spectra of covalently linked porphyrin-nitrobenzene compounds. J Phys Chem 1993;97:3974–3977.
11. Bell SEJ, Al-Obaidi AHR, Hegart MJN, McGarvey JJ, Hester RE. Resonance Raman spectra of the triplet state of free-base tetraphenylporphyrin and six of its isotopomers. J Phys Chem 1995;99:3959.
12. Woolley PS, Keely BJ, Bester RE. Surface-enhanced resonance Raman spectra of water-insoluble tetraphenylporphyrin and chlorophyll a on silver hydrosols with a dioxane molecular spacer. Chem Phys Lett 1996;258:501.
13. Unger E, Lipski RJ, Dreybrodt W, Schweitzer-Stenner R. Method for the evaluation of normal modes and molecular mechanics with reduced sets of force constants. 1. principles and reliability test. J Raman Spectrosc 1999;30:3–28.
14. Li XY, Zgierski MZ. Porphine force field: in-plane normal modes of free-base porphine. Comparison with metalloporphines and structural implications. J Phys Chem 1991;95:4268–4287.
15. Frisch MJ, Trucks GW, Schlegel HB, Scuseria GE, Robb MA, Cheeseman JR, Zakrzewski VG, Montgomery JA, Stratmann RE, Burant JC, Dapprich S, Millam JM, Daniels AD, Kudin KN, Strain MC, Farkas O, Tomasi J, Barone V, Cossi M, Cammi R, Mennucci B, Pomelli C, Adamo C, Clifford S, Ochterski J, Petersson GA, Ayala PY, Cui Q, Morokuma K, Malick DK, Rabuck AD, Raghavachari K, Foresman JB, Cioslowski J, Ortiz JV, Stefanov BB, Liu G, Liashenko A, Piskorz P, Komaroni I, Gomperts R, Martin RL, Fox DJ, Keith T, Al-Laham MA, Peng CY, Nanayakkara A, Gonzales C, Challacombe M, Gill PMW, Johnson BG, Chen W, Wong MW, Andres JL, Head-Gordon M, Replogle ES, Pople JA. Gaussian 98, revision A.3; Gaussian, Inc.: Pittsburgh, PA; 1998.
16. Becke AD. Density-functional thermochemistry. III. The role of exact exchange. J Chem Phys 1993;98:5648–5652.
17. Perdew JP, Wang Y. Accurate and simple analytic representation of the electron–gas correlation energy. Phys Rev B 1992;45:13244–13249.
18. Devlin FJ, Stephens PJ. Ab initio density functional theory study of the structure and vibrational spectra of cyclohexanone and its isotopomers. J Phys Chem A 1999;103:527–538.
19. Devlin FJ, Stephens PJ, Cheeseman JR, Frisch MJ. Prediction of vibrational circular dichroism spectra using density functional theory: camphor and fenchone. J Am Chem Soc 1996;118:6327–6328.
20. Bouř P, Sopková J, Bednárová L, Maloň P, Keiderling TA. Transfer of molecular property tensors in cartesian coordinates: A new algorithm for simulation of vibrational spectra. J Comput Chem 1997;18:646–659.
21. Hamor MJ, Hamor TA, Hoard JL. The structure of crystalline tetraphenylporphine. The stereochemical nature of porfine skeleton. J Am Chem Soc 1964;86:1938–1942.
22. Silvers SJ, Tulinski A. The crystal and molecular structure of triclinic tetraphenylporphyrin. J Am Chem Soc 1967;89:3331–3337.
23. Malsch K, Roeb M, Karuth V, Hohlneicher G. The importance of electron correlation for the ground state structure of porphycene and tetraoxaporphyrin-dication. Chem Phys 1998;227(3):331–348.
24. Bouř P, McCann J, Wieser H. Measurement and calculation of absolute rotational strengths for camphor, α-pinene and borneol. J Phys Chem A 1998;102:102–110.
25. Tam CN, Bouř P, Keiderling TA. Vibrational optical activity of (3S, 6S)-3,6-dimethyl-1,4-dioxane-2,5-dione. J Am Chem Soc 1996;118: 10285–10293.

26. Bouř P, Tam CN, Shaharuzzaman M, Chickos JS, Keiderling TA. Vibrational optical activity study of trans-d2-succinic anhydride. J Phys Chem 1996;100:15041–15048.
27. Barron LD. Molecular light scattering and optical activity. Cambridge: Cambridge University Press; 1982.
28. A Stein P, Ulman A, Spiro TG. Resonance Raman spectra of S_2TPP, SSeTPP, Se_2TPP, and H_2TPP: extended tetraphenylporphine vibrational assignments and bonding effects. J Phys Chem 1984;88:369–374.
29. Gurrieri S, Aliffi A, Bellacchio E, Laureci R, Purrelo R. Spectroscopic characterization of porphyrin supramolecular aggregates on polylysine and their application to quantitative DNA determination. Inorg Chim Acta 1999;286:121–126.
30. Bouř P, Keiderling TA. Computational evaluation of the coupled oscillator model in the vibrational circular dichroism of selected small molecules. J Am Chem Soc 1992;114:9100–9105.
31. Keiderling TA. In Fasman GD, editor. Circular dichroism and the conformational analysis of biomolecules. New York: Plenum; 1996. p 555–598.
32. Bouř P, Keiderling TA. *Ab initio* simulations of the vibrational circular dichroism of coupled peptides. J A Chem Soc 1993;15:9602–9607.